BROADENING THE IMAGING PHENOTYPE OF DYSFERLINOPATHY AT DIFFERENT DISEASE STAGES

JORGE DÍAZ, MD,[1] LISANNE WOUDT, MSc,[2] LIONEL SUAZO, MD,[1] CRISTIÁN GARRIDO, MT,[1] PABLO CAVIEDES, MD, PhD,[3] ANA M. CÁRDENAS, PhD,[4] CLAUDIA CASTIGLIONI, MD,[5] and JORGE A. BEVILACQUA, MD, PhD[2,6]

[1] Centro de Imagenología, Hospital Clínico Universidad de Chile, Santiago, Chile
[2] Unidad Neuromuscular, Departamento de Neurología y Neurocirugía, Hospital Clínico Universidad de Chile (HCUCH), Santos Dumont 999, 2° piso, Sector E. Independencia 8380456, Santiago, Chile
[3] Programa de Farmacología Molecular y Clínica, ICBM, Facultad de Medicina, Universidad de Chile
[4] Centro Interdisciplinario de Neurociencia de Valparaíso, Facultad de Ciencias, Universidad de Valparaíso, Valparaíso, Chile
[5] Unidad de Neurología, Departamento de Pediatría, Clínica Las Condes, Santiago, Chile
[6] Programa Anatomía y Biología del Desarrollo, ICBM, Facultad de Medicina, Universidad de Chile, Santiago, Chile

Accepted 12 January 2016

ABSTRACT: *Introduction:* MRI characterization of dysferlinopathy has been mostly limited to the lower limbs. We aimed to broaden the MRI description of dysferlinopathy and to correlate it with objective measures of motor dysfunction. *Methods:* Sequential whole-body axial MRI was performed in 27 patients with genetically confirmed dysferlinopathy classified according to disease duration. Spearman correlations of fatty infiltration scores versus Motor Function Measure (MFM) were calculated. *Results:* Significant fatty infiltration was symmetrically present in early stages mainly in the posterior compartments of legs and thighs, thigh adductors, pelvic girdle, and some paravertebral muscles and the subscapularis. Later, fatty infiltration involved leg and thigh anterior compartments, arms and forearms, paravertebral, and trunk muscles. MRI infiltration score correlated positively with disease duration and negatively with MFM scale. *Conclusions:* We expand MRI characterization of dysferlinopathy and provide evidence for use of MRI scoring combined with motor functional scales to assess the natural course of disease.

Muscle Nerve **54**: 203–210, 2016

Limb girdle muscular dystrophy type 2B (LGMD2B, OMIM#253601), Miyoshi myopathy (MM, OMIM#254130), and distal myopathy with anterior tibialis onset (DMAT, OMIM#606768) are the main clinical phenotypes associated with dysferlin gene (*DYSF*, MIM*603009) mutations.[1–4] Previous imaging reports of dysferlinopathy by computed tomography[5–7] and magnetic resonance imaging (MRI)[7–13] have shown early and more severe involvement of the posterior compartments of thighs and legs, which is independent of clinical phenotype.[13] Additionally, early imaging alterations in asymptomatic patients[14] and unusual patterns of muscle involvement have been described.[12,15,16] With the exception of Kesper et al., 2009[17] and Tasca et al., 2014,[18] these studies were focused on the lower limbs, and only 1 correlated MRI findings with the level of motor impairment progression, measured by means of a manual muscle testing composite based on the Medical Research Council scale (MRC).[13]

Recently, using 3 different functional scales, we established a correlation between motor functional testing and disease duration in a group of patients with genetically confirmed dysferlinopathy.[19] To complete the analysis, we reviewed the pattern of muscle involvement by whole-body MRI in 27 patients at different disease stages and correlated the findings with the level of functional impairment assessed by the Motor Function Measure scale.[20]

Abbreviations: DDG, disease duration group; DMAT, Distal myopathy with anterior tibial onset; DYSF, human dysferlin gene; FOV, field of view; LGMD2A, Limb girdle muscular dystrophy type 2A; LGMD2B, Limb girdle muscular dystrophy type 2B; MRI, magnetic resonance imaging; MFM, Motor Function Measure Scale; MM, Miyoshi's myopathy; MRC, Medical Research Council; MRS, Modified Rankin Scale; STIR, short tau inversion recovery.
Additional supporting information may be found in the online version of this article

Key words: clinical trials; dysferlinopathy; motor function measure; MRI; muscle disease; whole-body MRI
Funding: Supported by Grant FONDECYT#1110159, FONDECYT#1151383 and Grant Anillos #ACT1121 from the Comisión Nacional de Investigación Científica y Tecnología de Chile (CONICYT), Grant ENL15/14, from the Vicerrectoría de Investigación y Desarrollo, Universidad de Chile.

Disclosures: J. Díaz, L. Woudt, L. Suazo, C. Garrido, P. Caviedes, A. Cárdenas, and C. Castiglioni report no disclosures. Dr. Bevilacqua serves as Medical Advisor for neuromuscular diseases and myology for Genzyme Chile; and as Consultant and Coordinator of the Chilean Pompe Registry, GENZYME Chile Ltda. and has been invited to the 6th and 7th Dysferlin Conference with support from Jain Foundation Inc.

Correspondence to: J. A. Bevilacqua; jbevilac@med.uchile.cl

Published online 26 May 2016 in Wiley Online Library (wileyonlinelibrary.com).
DOI 10.1002/mus.25045

MATERIALS AND METHODS

Patients. Between 2011 and 2014, a total of 27 dysferlinopathy patients underwent sequential whole-body MRI and were evaluated clinically at the Department of Neurology and Neurosurgery of the Hospital Clínico Universidad de Chile (HCUCH), Santiago, Chile. The Ethics Committee of HCUCH and the Chilean National Commission of Scientific Research and Technology (CONICYT) approved the study protocol, and all patients gave informed consent.

All patients were symptomatic, and diagnosis was confirmed by direct DNA sequencing. Patient Dysf#001 was reported previously.[21] The clinical and genetic data of the cohort have been published

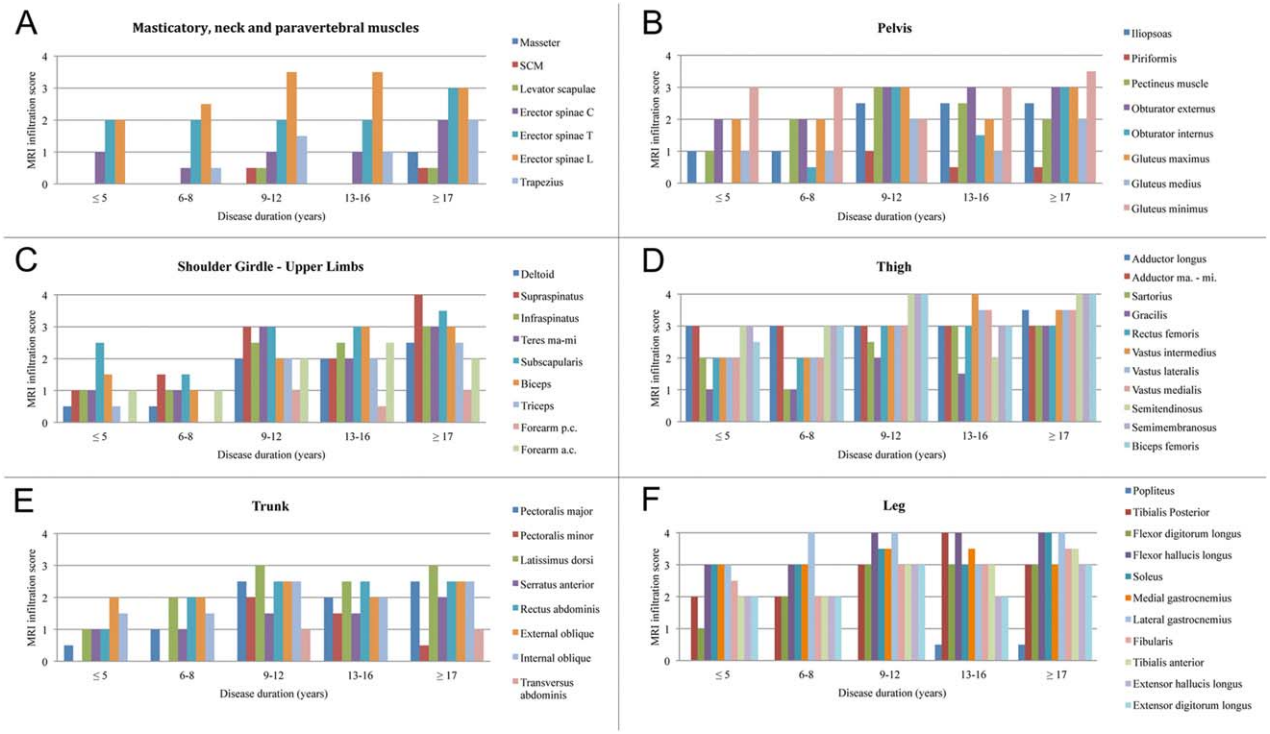

FIGURE 1. A–F: Graphic representation of the degree of fatty infiltration in individual muscles in each body segment according to disease duration groups (DDG). Charts are divided according to body segments, and each set of bars corresponds to a DDG. Every colored bar represents the averaged median of the fatty infiltration score from both evaluators of all patients in the DDG and from both body sides for the indicated muscle. Overall, there was an increase in fatty infiltration scores according to disease duration, but some muscles occasionally showed lower scores with longer disease duration (for example, see gracilis in D). Some muscles were already severely affected in DDG1 (for example, medial gastrocnemius, adductors, gluteus minimus, lumbar paravertebral, and subscapularis), even in the patient with the shortest disease duration (Dysf#23). No individual muscle could be identified as a timeline marker of disease progression with this method.

elsewhere[19] and are summarized in Supplementary Table S1, available on line.

Irrespective of clinical phenotype, the 27 patients were classified into 5 groups according to disease duration (DDGs) at the time of MRI: DDG1, ≤ 5 years ($n = 5$); DDG2, 6–8 years ($n = 7$); DDG3, 9–12 years ($n = 5$); DDG4, 13–16 years ($n = 5$); and DDG5, > 17 years ($n = 5$) (Supp. Table S1, available online).

MRI. Images were acquired using a 1.5 Tesla (T) system (Magnetom Symphony Maestro-Class, Siemens, Erlangen, Germany).[22,23] Patients were scanned from temporal to ankle levels in the supine position, with the arms alongside the body. The protocol included axial T1-weighted (T1W) spin-echo (repetition time [TR]: 610–640 ms, echo time [TE]: 11–12 ms) and T2 short-time inversion recovery (STIR) (TR: 3700–4500 ms, TE: 51–64 ms, TI: 150) sequences. The study protocol usually included 5 slabs of 30 slices. There were no gaps between the slabs. The slice thickness was 8 mm with a interslice gap of 4 mm. The field of view (FOV) was between 350 and 490 mm, with a matrix of approximately 384×240. Total time in the MRI room averaged 45 min. Additionally, upper limbs from 5 representative patients were evaluated separately with a smaller FOV. MRI scans were analyzed with DICOM OsiriX viewer by 2 experienced and independent musculoskeletal radiologists (J.D. and L.S.) who were blinded to the patients' clinical and genetic data. The degree of fatty infiltration and muscle bulk (atrophy/hypertrophy) was evaluated in T1W images; STIR sequences were used to assess the presence or absence of muscle edema.

Fatty infiltration was scored according to the scale adapted by Kornblum et al. 2006.[24] A list of the muscles analyzed is depicted in Supplementary Table S2. The degree of fatty infiltration was described as follows: none (0), mild (1), moderate (2a), moderate to severe (2b), and severe (3), and the values were transformed to score numbers (0 = score 0; 1 = score 1; 2a = score 2; 2b = score 3; and 3 = score 4), for statistical purposes.

Median MRI scores from both evaluators were averaged for individual muscles in the different DDGs and were separated into left- and right-sided. Values were represented as bar-graphs for individual muscles in each body segment (Fig. 1).

Functional Assessment. Motor disability was determined as described in a previous report[19] using the Motor Function Measure (MFM) scale,[20] Modified

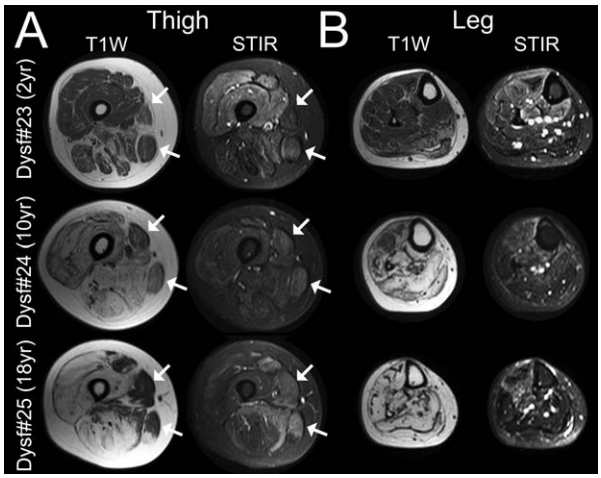

FIGURE 2. MRI of the Lower Limb. Representative axial T1W and STIR images of thighs (**A**) and legs (**B**), of patients in DDG1, 3, and 5. The posterior compartments of legs and thighs are clearly infiltrated by fat early in the disease. Muscles with no fat replacement in the anterior compartments of legs and thighs show edema and reach a similar level of involvement as in the posterior compartment at later stages. The sartorius and gracilis remain relatively spared in the thighs, but as shown in the lower row, at 18 years of disease course, these spared muscles also show edema (arrows). In general, edema tends to decrease with disease progression.

Rankin Scale (MRS),[25] and MRC score[26] (Supp. Table S1). MFM (n = 25) was performed by the same examiners (C.C. and J.A.B.) within the same week of the MRI acquisition in each patient, and results are expressed as a percentage of the maximum possible score. Percentage of inter-observer agreement was 93.56% ± 6.54 SD. Patients Dysf#19 and Dysf#20 did not accomplish MFM. MRI data were compared with MFM scale scores only in the 25 patients who completed both, MFM and MRI (Supp. Table S1).

Statistical Analysis. Spearman correlation was used to describe the association between quantitative variables. Two-tailed *t*-tests or Mann-Whitney *U*-tests were used for comparative analysis between phenotype groups. IBM SPSS Statistics 21 (New York: IBM Corp., 2012) was used for all analyses.

RESULTS

Clinical and MRI Findings. Main clinical and genetic features of the patients, and scoring of MFM functional scale are summarized in Supplementary Table S1. Figure 1 shows the degree of individual muscle involvement in each DDG. Fatty infiltration was mainly symmetrical in most muscles included (Supp. Fig. S1A). No statistical differences were found on MRI findings between MM or LGMD2B phenotypes (Supp. Fig. S1). T1W and STIR MRI images of representative patients are shown in Figures 2–4. Disease duration correlated with total MFM score ($r = -0.72$; $P < 0.001$) (Fig. 5A) and with MRI fatty infiltration score ($r = 0.62$; $P < 0.001$) (Fig. 5B). Furthermore, a negative correlation was found for MRI fatty infiltration level versus global MFM score ($r = -0.57$; $P < 0.003$) (Fig. 5C) and MFM-D1 subscore ($r = -0.59$; $P < 0.002$) (Fig. 5D).

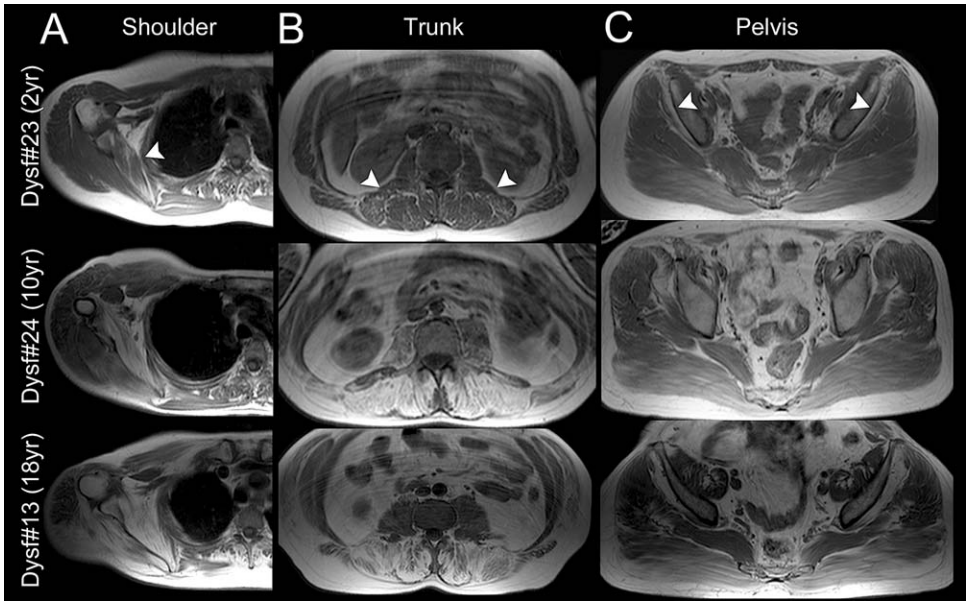

FIGURE 3. MRI of the shoulder (**A**), trunk (**B**), and pelvis (**C**). Axial T1W images of shoulder girdle, trunk, and pelvis of representative DDG1, 3, and 5 patients. The subscapularis, lumbar erector spinae, and gluteus minimus present with early involvement. Muscle involvement progresses to most remaining muscles according to disease duration. Arrowheads indicate the leading affected muscle in each segment. A, subscapularis, B, lumbar erector spinae; C, gluteus minimus.

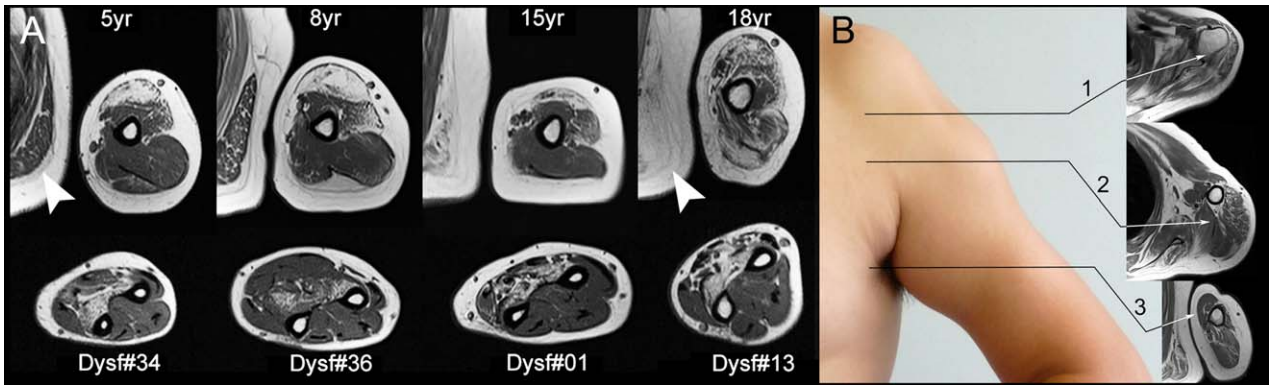

FIGURE 4. MRI of the Upper Limb. **A**: Focused upper limb axial T1W images from representarive patients of 4 DDGs. The anterior compartments of arms and forearms are more affected than the posterior compartments. In early stages, the first involved muscles are the long head of biceps in the arm and flexor digitorum profundus in the forearm. Note involvement of the posterior compartment of the arm (triceps) at later stages (Dysf#13, 18 years of disease), and progressive involvement of the latissimus dorsi (arrowhead). **B**: Correlation of clinical and MRI findings. The depressed area in the proximal third of the arm seems to be explained by lower volume of the deltoid muscle (B1). The focal bulging at the lower deltoid area corresponds to a preserved portion of the deltoid (B2), as the relative sparing of the short head of the biceps brachialis and coracobrachialis (B2) would explain the apparent bulging of the superior internal third of the anterior compartment of the arm (B3).

Description of Findings by Body Segments, according to DDGs. Representative T1W and STIR images of body segments studied at different times of disease are shown in Figures 2, 3 and 4.

Legs. The muscles of the posterior compartment (soleus and medial and lateral gastrocnemius) and flexor hallucis longus were the first to be involved. They showed moderate to severe fatty infiltration in early stages (DDG1) and reached complete fatty replacement at end stages of the disease (DDG5). The medial gastrocnemius showed a lesser degree of progression of involvement.

The anterior compartment and fibularis muscles showed moderate involvement initially and reached moderate to severe abnormality from 9 years of disease until to the end stage (DDG3–DDG5).

In the central compartment, the tibialis posterior and flexor digitorum longus have a relatively similar degree of fatty infiltration as compared to the anterior compartment along the whole evolution of the disease. The popliteus was spared throughout the disease course (not shown).

In early stages, edema is present only in the soleus in the posterior compartment, but it disappears later. In the anterior compartment and fibularis muscle, edema increases until 8 years of disease (DDG2), persists only in the anterior compartment between 13 and 16 years (DDG4), and disappears afterward (data not shown).

Thighs. In the first 5 years of disease (DDG1), the hamstrings and adductors were more affected than the quadriceps, showing moderate to severe fatty infiltration. After 9 years of disease (DDG3), the quadriceps and adductors showed moderate to severe changes, and the hamstrings reached end stage, with relative sparing of the sartorius and gracilis. At end-stage disease (DDG5), we observed a similar pattern of abnormality of the different compartments, identifying only a small amount of progression in the quadriceps, adductors, sartorius, and gracilis.

Edema was observed in practically all thigh muscles in early-stage disease and gradually decreased with disease progression. At end stage (DDG5), we identified edema only in adductors, sartorius, gracilis, rectus femoris, and vastus lateralis (Fig. 2).

Pelvis. The gluteus minimus is the most affected muscle in early stages, showing moderate to severe fatty replacement until 8 years of disease (DDG1 and DDG2), followed by pectineus and obturator externus. The piriformis and internal obturator were spared. At DDG3, fatty infiltration was remarkably greater in the iliopsoas, pectineus, obturator externus and internus, and gluteus maximus, with progression to moderate to severe abnormality.

At later disease stages (DDG4 and DDG5), there was severe fatty infiltration of gluteus minimus. The obturator externus and internus and the gluteus maximus showed moderate to severe fatty infiltration. The gluteus medius showed lesser involvement, and the piriformis was relatively unaffected at all disease stages. Assessment of the gluteus maximus was difficult due to the normal presence of multiple fat spots.

Early edema was observed in the iliopsoas, gluteus maximus, pectineus, and obturator externus, but not in the gluteus minimus. The edema decreased with disease progression, persisting only in the obturator externus in the 13–16 year group (DDG4); after 17 years of disease, edema disappeared.

Trunk. Overall, fatty degeneration of trunk muscles was less severe than that of muscles of the

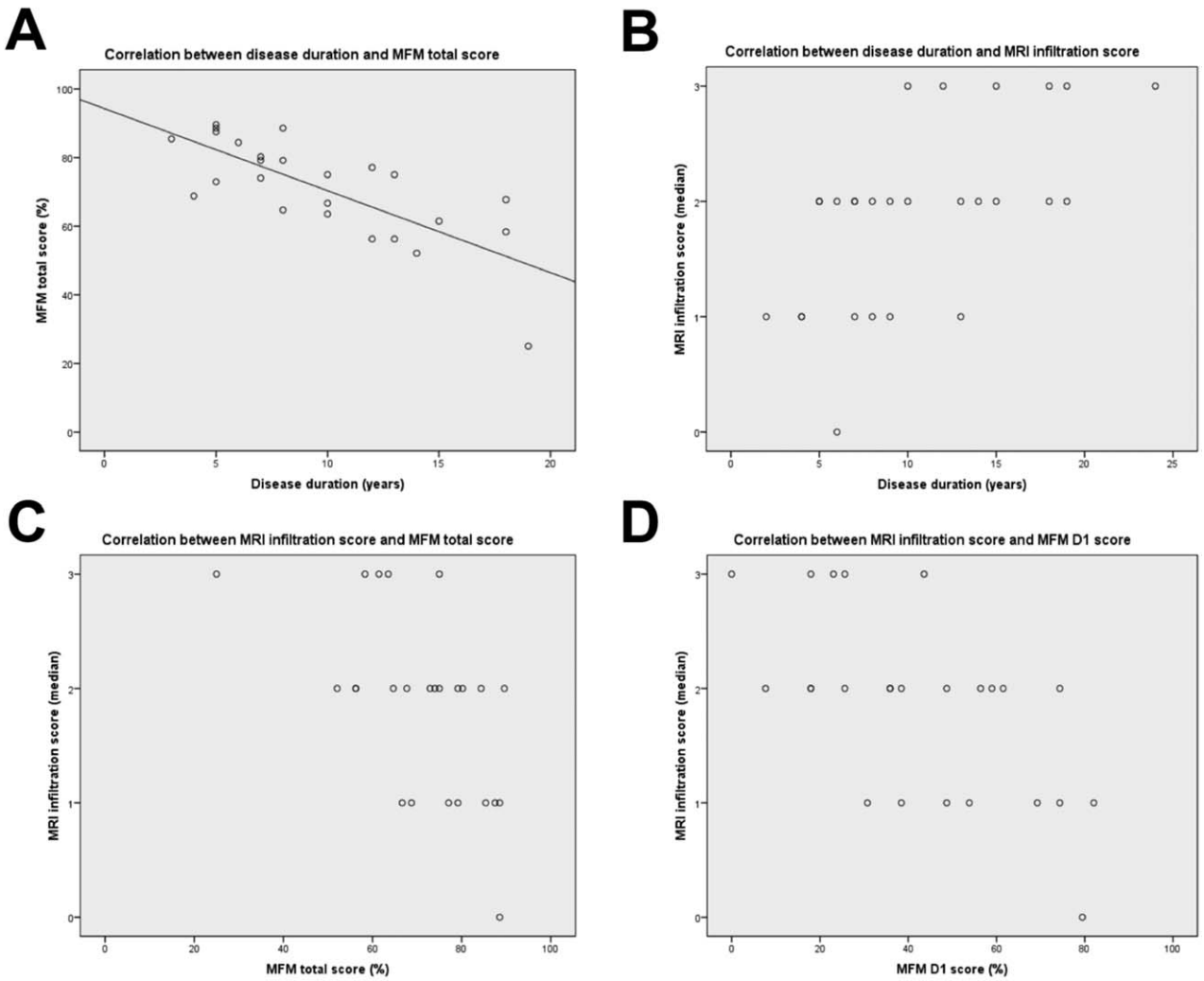

FIGURE 5. Spearman correlations for disease duration versus MFM scores and MRI infiltration; and MRI fatty infiltration scores versus disease duration and MFM scores. Scatterplot representation of Spearman correlations between disease duration versus total MFM score ($r = -0.72$; $P < 0.001$) **(A)**; disease duration versus MRI fatty infiltration score ($r = 0.62$; $P < 0.001$) **(B)**; MFM total score versus MRI fatty infiltration score ($r = -0.57$; $P < 0.003$) **(C)**, and MFM-D1 subscore versus MRI infiltration score ($r = -0.59$; $P < 0.002$) **(D)**. D1 score is more representative of disease progression than the other MFM D2 and D3 subscores. According to disease duration, the motor score measured with MFM decreases (A), as the fatty infiltration score assessed with MRI increases (B). Global MFM score correlated negatively with MRI infiltration score (C), this was better represented using only dimension 1 (D1) of the MFM scale (D), thus demonstrating that as fatty infiltration score increases, motor function decreases.

lower limbs and pelvis. In DDG1, the external and internal obliques were the first affected muscles, showing moderate fatty replacement in early disease. After 5 years of disease (DDG2) latissimus dorsi, rectus abdominis, and external oblique muscles showed moderate involvement. Between 9 and 12 years of disease (DDG3), moderate to severe changes were seen in the pectoralis major, latissimus dorsi, rectus abdominis, and external and internal oblique, with comparatively less involvement of the pectoralis minor.

The rectus abdominis, external and internal obliques, pectoralis major, and latissimus dorsi all showed moderate to severe fatty infiltration at end-stage disease (DDG5). Pectoralis minor was only mildly involved. Findings of the thoracic and abdominal segments must be interpreted cautiously due to motion artifacts.

In DDG1, edema was found in the latissimus dorsi and rectus abdominis, but these muscles did not show edema in the other groups. Between 6 and 12 years of disease (DDG2–DDG3), edema is observed in the pectoralis major and the external oblique, but not at later disease stages.

Shoulder Girdle and Upper Limbs. The subscapularis was the first affected muscle in the shoulder girdle, showing moderate involvement in early stages. The supraspinatus, infraspinatus, teres major-minor, and anterior compartments of the arm and forearm presented mild changes in the DDG1.

In DDG3 the supraspinatus, teres major-minor, and subscapularis showed moderate to severe fatty infiltration, while the deltoid, infraspinatus, biceps, triceps, and the anterior compartment of the forearm had moderate abnormality.

In end-stage disease (DDG5), both the subscapularis and supraspinatus muscles reached severe fatty infiltration. The infraspinatus, teres major-minor, deltoid, biceps, and triceps showed moderate to severe involvement. In the forearms, we observed moderate fatty infiltration of the anterior compartment. The posterior compartments of the forearms were relatively spared throughout the disease course.

MRI analysis of the upper limbs showed more severe involvement of the long head of the biceps than the short head, with relative sparing of the coracobrachialis. The triceps showed moderate involvement, predominantly in the long head. In the forearms, the brachioradialis and the anterior compartment (especially the flexor digitorum profundus and flexor pollicis longus), were the most affected muscles. The posterior (extensor) compartment was mainly spared until late disease stages.

The supraspinatus, infraspinatus, teres major-minor, biceps, triceps, and anterior forearm compartment showed edema early that persisted until 12 years of disease, except for the biceps and triceps. After 13 years of disease, edema was only observed in the anterior forearm compartment.

Masticatory, Neck, and Paravertebral Muscles. Masticatory and neck muscles were mostly spared until end-stage disease. The masseter and sternocleidomastoid muscles showed mild involvement in end-stage disease (DDG5).

The lumbar and thoracic erector spinae were the most affected paravertebral muscles. Abnormality was moderate for both levels in early stages (DDG1). In DDG3 we observed moderate to severe fatty infiltration in lumbar paravertebral muscles and moderate at the thoracic level. The compromise was moderate to severe for both levels in end-stage disease (DDG5). Edema was not observed in masticatory and neck muscles; in the lumbar erector spinae it was present early, disappearing after 9 years of disease.

DISCUSSION

We performed sequential whole body and focused upper limb MRI in a cohort of 27 dysferlinopathy patients, comparing MM and LGMD2B phenotypes to look for correlation of MRI findings with disease duration and motor impairment. The division of patients according to disease duration, although made arbitrarily, provided us with 5 comparable groups. Gender, age, and phenotype distribution within groups were consistent, showing a significantly greater average age, only in DDG5 with longer disease course. Importantly, consistency of MFM score in each DDG was well reflected in the Spearman correlation (Fig. 5).

As reported earlier,[8,11–13,17,27,28] we observed that the posterior compartments of thighs and legs and thighs adductors in the lower limbs already had moderate to severe fatty infiltration at clinical onset, with a lesser degree of involvement of anterior and lateral compartments of the legs and the anterior compartments of the thighs. We can add that the flexor hallucis longus also shows early involvement. The gracilis and sartorius were comparatively less affected among thigh muscles. However, we were not able to find any particular pattern of temporal involvement of individual muscles in the different compartments as previously suggested.[13,17] As described in a previous report,[17] relatively earlier involvement of gluteus minimus in the pelvis was observed, but also of the pectineus and obturator externus (not described before), followed later by the iliopsoas. As reported earlier,[17,18] the shoulder girdle showed early involvement of the subscapularis followed by the supraspinatus and later by infraspinatus and teres major-minor.

We additionally found involvement of the biceps and triceps brachii and forearm flexors that was clearly present after 9 years of disease (Fig. 4). The long head of the biceps brachii, brachioradialis, flexor digitorum profundus, and flexor pollicis longus were the most affected muscles in the upper limb. These findings are in agreement with clinical observations. In the trunk, involvement of lumbar and thoracic erector spinae, and to a lesser degree of the latissimus dorsi, pectoralis major, and external oblique is in agreement with previous findings,[17] nonetheless involvement of the rectus abdominis and internal oblique was additionally demonstrated. As reported by Tasca et al.,[18] a lesser degree of fatty infiltration of trapezius and serratus anterior with sparing of levator scapulae are also confirmed. However, after 17 years of disease, these differences are no longer apparent, as most lower and upper limb muscles are diffusely replaced by fibroadipose tissue.

Edema precedes fatty replacement throughout the disease course (Fig. 2), anticipating which muscles would later undergo fatty replacement. It persists in some less affected muscles after 18 years of disease, indicating their involvement. A comparative analysis of MRI findings in dysferlinopathy with other forms of recessive LGMDs, demonstrates that the pattern of MRI involvement for LGMD2B is very similar to that described for LGMD2A, 2I, and 2L in thighs and legs, and

perhaps a consistent difference could be early fatty infiltration of gluteus minimus in LGMD2B. Unlike dysferlinopathies, sarcoglycanopathies tend to respect the legs and to affect predominantly the anterior compartments of the thighs.

In summary, although muscle involvement in dysferlinopathy has similarities with other recessive LGMDs,[22,27,29–31] it seems to have some distinctive features that roughly follow a sequence of events comprising: (1) early involvement of the posterior compartments of legs and thighs; (2) marked fatty replacement of gluteus minimus and lumbar erector spinae; (3) early and selective involvement of the subscapularis, followed in succession by the supraspinatus, infraspinatus, teres major-minor, anterior compartment of the arm and forearm; with (4) sparing of craniofacial muscles.

Although we analyzed a significant number of patients at different disease stages, these observations must be taken cautiously, because we could only infer the progression of muscle involvement by extrapolating data at different disease stages from different patients, thus a picture of disease progression in individual patients is not available. This is clearly a major limitation of our study to observe disease progression, for which a proper analysis can only be achieved by repeating MRI and functional testing in individual patients at different disease time-points. We are currently doing this in some representative patients of the cohort. An additional limitation of our approach is that we have only made a qualitative assessment of fatty replacement compared with functional measures.

In recent publications, quantitative methods have been shown to have greater discrimination in both cross-sectional[32] and longitudinal[33] studies compared with physical function tests and have reduced the acquisition times of these techniques.[34] The implementation of such methods will provide more sensitive measures of disease course and progression for future work. Nevertheless, until such data become available, we believe that this approach provides a fairly good panorama of how muscle involvement evolves in dysferlin-related myopathy.

The MRI fatty infiltration score correlated with both disease duration and MFM score, indicating that despite the limitations of the analysis, these parameters are consistently measurable, thus allowing noninvasive follow-up of the patients for any purpose that could be required.

In addition to the description of novel imaging features of dysferlinopathy, particularly in upper limbs, this study complements our previous observational report, based on the largest cohort of dysferlinopathy patients in Latin America[19] by adding evidence of the convenience of MRI assessment in combination with functional scales as reliable outcome measures potentially useful for longitudinal follow-up in dysferlinopathy.

We thank the patients and families for their generous participation and the colleagues that entrusted their patients to us. We thank Ms. Pilar Varas from the Centro de Imagenología, HCUCH and Ms. Marcela Ramírez, from the Departamento de Neurología y Neurocirugía, HCUCH for their assistance and coordination of the study. Thanks to Yamile A. Corredoira, MD, from the Department of Pathology, Universidad de Chile for reviewing the English version of the manuscript.

REFERENCES

1. Bashir R, Britton S, Strachan T, Keers S, Vafiadaki E, Lako M, et al. A gene related to Caenorhabditis elegans spermatogenesis factor fer-1 is mutated in limb-girdle muscular dystrophy type 2B. Nat Genet 1998;20:37–42.
2. Liu J, Aoki M, Illa I, Wu C, Fardeau M, Angelini C, et al. Dysferlin, a novel skeletal muscle gene, is mutated in Miyoshi myopathy and limb girdle muscular dystrophy. Nat Genet 1998;20:31–36.
3. Aoki M, Liu J, Richard I, Bashir R, Britton S, Keers SM, et al. Genomic organization of the dysferlin gene and novel mutations in Miyoshi myopathy. Neurology 2001;57:271–278.
4. Illa I, Serrano-Munuera C, Gallardo E, Lasa A, Rojas-García R, Palmer J, et al. Distal anterior compartment myopathy: a dysferlin mutation causing a new muscular dystrophy phenotype. Ann Neurol 2001;49:130–134.
5. Meola G, Sansone V, Rotondo G, Jabbour A. Computerized tomography and magnetic resonance muscle imaging in Miyoshi's myopathy. Muscle Nerve 1996;19:1476–1480.
6. Linssen WH, Notermans NC, Van der Graaf Y, Wokke JH, Van Doorn PA, Höweler CJ, et al. Miyoshi-type distal muscular dystrophy. Clinical spectrum in 24 Dutch patients. Brain 1997;120:1989–1996.
7. Park HJ, Hong JM, Suh GI, Shin HY, Kim SM, Sunwoo IN, et al. Heterogeneous characteristics of Korean patients with dysferlinopathy. J Korean Med Sci 2012;27:423–429.
8. Cupler EJ, Bohlega S, Hessler R, McLean D, Stigsby B, Ahmad J. Miyoshi myopathy in Saudi Arabia: clinical, electrophysiological, histopathological and radiological features. Neuromuscul Disord 1998;8:321–326.
9. Katz JS, Rando TA, Barohn RJ Saperstein DS, Jackson CE, Wicklund M, et al. Late-onset distal muscular dystrophy affecting the posterior calves. Muscle Nerve 2003;28:443–448.
10. Ro LS, Lee-Chen GJ, Lin TC, Wu YR, Chen CM, Lin CY, et al. Phenotypic Features and Genetic Findings in 2 Chinese Families With Miyoshi Distal Myopathy. Arch Neurol 2004;61:1594–1599.
11. Brummer D, Walter MC, Palmbach M, Knirsch U, Karitzky J, Tomczak R, et al. Long-term MRI and clinical follow-up of symptomatic and presymptomatic carriers of dysferlin gene mutations. Acta Myol 2005;24:6–16.
12. Illa I, De Luna N, Domínguez-Perles R, Rojas-García R, Paradas C, Palmer J, et al. Symptomatic dysferlin gene mutation carriers: characterization of two cases. Neurology 2007;68:1284–1289.
13. Paradas C, Llauger J, Díaz-Manera J, Rojas-García R, De Luna N, Iturriaga C, et al. Redefining dysferlinopathy phenotypes based on clinical findings and muscle imaging studies. Neurology 2010;75:316–323.
14. Okahashi S, Ogawa G, Suzuki M, Ogata K, Nishino I, Kawai M. Asymptomatic Sporadic dysferlinopathy presenting with elevation of serum creatine kinase. Typical distribution of muscle involvement shown by MRI but not by CT. Intern Med 2008;47:305–307.
15. Diers A, Carl M, Stoltenburg-Didinger G, Vorgerd M, Spuler S. Painful enlargement of the calf muscles in limb girdle muscular dystrophy type 2B (LGMD2B) with a novel compound heterozygous mutation in DYSF. Neuromuscul Disord 2007;17:157–162.
16. Seror P, Krahn M, Laforet P, Leturcq F, Maisonobe T. Complete fatty degeneration of lumbar erector spinae muscles caused by a primary dysferlinopathy. Muscle Nerve 2008;373:410–414.
17. Kesper K, Kornblum C, Reimann J, Lutterbey G, Schröder R, Wattjes MP. Pattern of skeletal muscle involvement in primary dysferlinopathies: a whole-body 3.0-T magnetic resonance imaging study. Acta Neurol Scand 2009;120:111–118.
18. Tasca G, Monforte M, Iannaccone E, Laschena F, Ottaviani P, Leoncini E, et al. Upper girdle imaging in facioscapulohumeral muscular dystrophy. PLoS One 2014;9:e100292.
19. Woudt L, Di Capua G, Khran M, Castiglioni C, Hughes R, Campero M, et al. Toward an objective measure of functional disability in dysferlinopathy. Muscle Nerve Epub 2016;53:49–57.

20. Bérard C, Payan C, Hodgkinson I, Fermanian J. The MFM Collaborative Study Group. A motor function measure for neuromuscular diseases. Construction and validation study. Neuromuscul Disord 2005;15:463–470.
21. Bevilacqua JA, Krahn M, Pedraza L, Gejman R, Gonzalez S, Lévy N. Dysferlinopathy in Chile evidence of two novel mutations in the first reported cases. Genet Test Mol Biomarkers 2009;13:105–108.
22. Fischer D, Walter MC, Kesper K, Petersen JA, Aurino S, Nigro V, et al. Diagnostic value of muscle MRI in differentiating LGMD2I from other LGMDs. J Neurol 2005;252:538–547.
23. Mercuri E, Pichiecchio A, Counsell S, Allsop J, Cini C, Jungbluth H, et al. A short protocol for muscle MRI in children with muscular dystrophies. Eur J Paediatr Neurol 2002;6:305–307.
24. Kornblum C, Lutterbey G, Bogdanow M, Kesper K, Schild H, Schröder R, et al. Distinct neuromuscular phenotypes in myotonic dystrophy types 1 and 2: a whole body highfield MRI study. J Neurol 2006;253:753–761.
25. van Swieten JC, Koudstaal JP, Visser MC, Schouten HJA. Interobserver agreement for the assessment of handicap in stroke patients. Stroke 1988;19:604–607.
26. Medical Research Council. Aids to the examination of the peripheral nervous system, Memorandum No. 45. London: Her Majesty's Stationery Office; 1981.
27. Stramare R, Beltrame V, Dal Borgo R, Gallimberti L, Frigo AC, Pegoraro E, et al. MRI in the assessment of muscular pathology: a comparison between limb-girdle muscular dystrophies, hyaline body myopathies and myotonic dystrophies. Radiol Med 2010;115:585–599.
28. Angelini C, Peterle E, Gaiani A, Bortolussi L, Borsato C. Dysferlinopathy course and sportive activity: clues for possible treatment. Acta Myol 2011;30:127–132.
29. Mercuri E, Bushby K, Ricci E, Birchall D, Pane M, Kinali M, et al. Muscle MRI findings in patients with limb girdle muscular dystrophy with calpain 3 deficiency (LGMD2A) and early contractures. Neuromuscul Disord 2005;15:164–171.
30. Mercuri E, Jungbluth H, Muntoni F. Muscle imaging in clinical practice: diagnostic value of muscle magnetic resonance imaging in inherited neuromuscular disorders. Curr Opin Neurol 2005;18:526–530.
31. Sarkozy A, Deschauer M, Carlier RY, Schrank B, Seeger J, Walter MC, et al. Muscle MRI findings in limb girdle muscular dystrophy type 2L. Neuromuscul Disord 2012;22(Suppl 2):S122–S129.
32. Willis TA, Hollingsworth KG, Coombs A, Sveen ML, Andersen S, Stojkovic T, et al. Quantitative magnetic resonance imaging in limb-girdle muscular dystrophy 2I: a multinational cross-sectional study. PLoS One 2014;9:e90377.
33. Willis TA, Hollingsworth KG, Coombs A, Sveen ML, Andersen S, Stojkovic T, et al. Quantitative muscle MRI as an assessment tool for monitoring disease progression in LGMD2I: a multicentre longitudinal study. PLoS One 2013;8:e70993.
34. Loughran T, Higgins DM, McCallum M, Coombs A, Straub V, Hollingsworth KG. Improving highly accelerated fat fraction measurements for clinical trials in muscular dystrophy: origin and quantitative effect of R2* changes. Radiology 2015;275:570–578.